Systematic Frequency Error in Laser Synchronization Circuits for Fiber-Optic Time-Transfer Systems

Ł. Śliwczyński, *Member, IEEE*, P. Krehlik, Ł. Buczek, and H. Schnatz

***Abstract*—This article addresses the problem of a systematic frequency error occurring in semiconductor-laser frequency synchronization circuits based on counting the beat note between the two lasers in a reference time interval using a high-frequency prescaler. Such synchronization circuits are suitable for operation in ultraprecise fiber-optic time-transfer links, used, e.g., in time/frequency metrology. The error occurs when the power of the light coming from the reference laser, to which the second laser is synchronized, is below about −50 to −40 dBm, depending on the details of particular circuit implementation. The error can reach tens of megahertz if left out of consideration and does not depend on the frequency difference between the synchronized lasers. Its sign can be positive or negative, depending on the spectrum of the noise at the prescaler input and the frequency of the measured signal. In this article, we present the background of the systematic frequency error, discuss important parameters allowing for predicting the error value, and describe the simulation and theoretical models being helpful for designing and understanding operation of discussed circuits. The theoretical models presented here show good agreement with the experimental data, which demonstrates the usefulness of the proposed methods. Implementing polarization scrambling to mitigate the effect of polarization misalignment of the lights of the lasers used was considered and the resulting penalty was determined.**

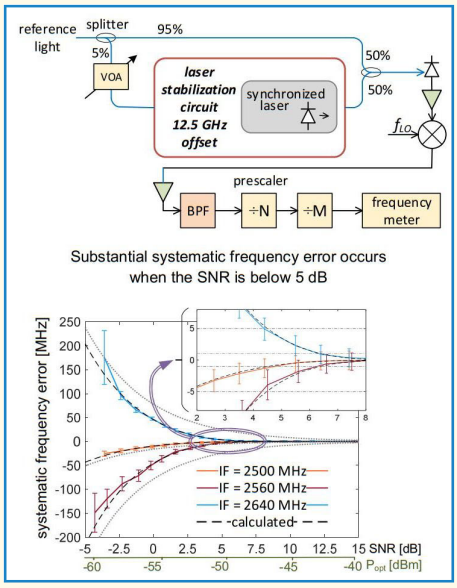

***Index Terms*—Calibration uncertainty, fiber optic, frequency prescaler, laser frequency synchronization, systematic frequency error, time transfer.**

I. Introduction

FIBER-OPTIC time and frequency (T&F) transfer starts to become a well-established technology that can be used not only to compare clocks in the optical domain but also to distribute timescales from nated universal time (UTC) laboratories to distant users. Apart from metrology laboratories and those involved directly in time, frequency, or metrology activities [1], [2], [3], the applications include a broad range of scientific cases, e.g., spectroscopy [4], astronomy [very long baseline interferometry (VLBI)] [5], [6], [7], or geodesy [8]. Due to the high stability and accuracy possible by fiber-optic transfer, there is also a growing number of sensitive commercial applications, such as in telecommunication [9], [10], navigation and positioning [11], and smart grids [12], or in the financial sector [13], where a certain amount of independency from global navigation satellite systems (GNSS), ubiquitously used for T&F transfer, is important [14].

A simplified schematic of a fiber-optic time-transfer link with stabilized propagation delay is shown in Fig. 1. Apart from a set of local and remote fiber-optic transmitters (TX) and receivers (RX), it includes a delay compensation system, which can be realized using a pair of matched variable electronic delay lines [15] or, in some cases, variable optical delays [16]. The optical TX needs to use different wavelengths (λ_A and λ_B) to allow filtering out the undesired optical signals

Manuscript received 2 November 2022; accepted 13 February 2023. Date of publication 14 February 2023; date of current version 28 March 2023. This work was supported by the Polish National Science Center under Grant 2017/26/M/ST7/00128. *(Corresponding author: Ł. Śliwczyński.)*

Ł. Śliwczyński, P. Krehlik, and Ł. Buczek are with the Department of Computer Science, Electronics and Telecommunications, AGH University of Science and Technology, 30-059 Kraków, Poland (e-mail: sliwczyn@agh.edu.pl; krehlik@agh.edu.pl; lbuczek@agh.edu.pl).

H. Schnatz is with the Division of Quantum Optics and Unit of Length, Physikalisch-Technische Bundesanstalt (PTB), 38116 Braunschweig, Germany (e-mail: har-ald.schnatz@ptb.de).

Digital Object Identifier 10.1109/TUFFC.2023.3245289

Highlights

- **A systematic frequency error occurs in the laser synchronization circuits because of a narrow-band noise present at the input of the prescaler used to divide down the beat note frequency.**
- **The models proposed in the text help to understand an analyze the problem, giving a tool to predict the value of the frequency error.**
- **Developed tools and theory will help design and implementation of picosecond-accurate long-distance fiber-optic time transfer systems using laser transmitters synchronized to weak incoming light.**

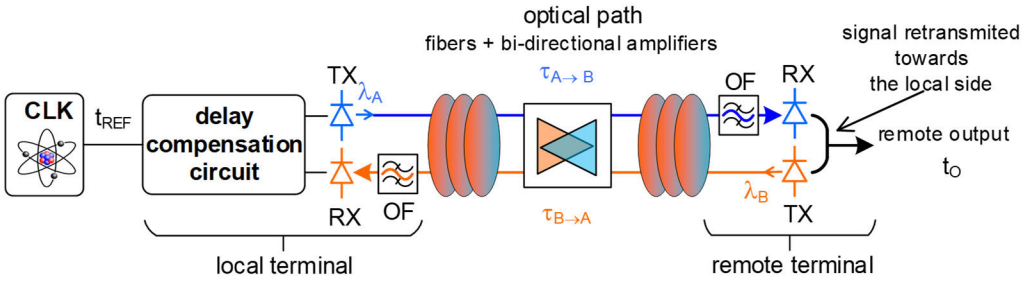

Fig. 1. Simplified diagram of a stabilized time-transfer fiber-optic link. OF: optical filter.

resulting from Rayleigh backscattering [17] and reflections. In such a link, the timescale t_0 transferred to the remote end of the link can be expressed as

$$t_0 = t_{\mathrm{REF}} - T_{\mathrm{RT}}/2 - \Delta\tau_{AB}/2 \tag{1}$$

where T_{RT} is the round-trip propagation delay of the link and $\Delta\tau_{A\leftrightarrow B} = \tau_{A\to B} - \tau_{B\to A}$ is the link asymmetry being the difference of the forward ($\tau_{A\to B}$) and backward (τ_{BA}) propagation delays of the link. The link asymmetry can be further decomposed into

$$\Delta\tau_{A\leftrightarrow B} = \Delta\lambda_{A\leftrightarrow B} D_T + \tau_{\mathrm{Sagnac}} + \tau_{\mathrm{pol}} + \tau_C \tag{2}$$

where the first term is related to the chromatic dispersion of the fiber ($\Delta\lambda_{A\leftrightarrow B}$ is the wavelength difference of the local and remote lasers and D_T is the chromatic dispersion accumulated along the fiber), τ_{Sagnac} is the Sagnac correction [18], τ_{pol} is related to the polarization dispersion, and τ_C is the correction related to the asymmetry of propagation inside the local and remote terminals.

For an accurate time transfer, it is essential to know both T_{RT} and $\Delta\tau_{A\leftrightarrow B}$ with low uncertainties. This is not a problem for the round-trip delay, which requires only a time interval measurement and can be realized with a few picoseconds uncertainty (see [19]). In the case of link asymmetry, however, the uncertainty depends also on the accuracy of the wavelengths of the lasers and the accuracy of determining the accumulated chromatic dispersion D_T. The uncertainty contribution related to this term may be large and can reach tens of picoseconds for long links [9].

A possible solution to this problem is to use one of the lasers (e.g., from the local terminal of the transfer system) as a source of the reference light and stabilize the wavelength of the second laser to this wavelength with a desirable offset [20]. In hybrid systems, transferring jointly stable optical frequency and time [21], [22], [23], [24], this ultrastable optical frequency can also be used as a source of reference light. Using this approach, the uncertainty contribution can be reduced to a single picosecond level, even for 1000-km-long links, which requires uncertainty of the lasers' relative frequency lower than about 5 MHz (see [25] for detailed discussion).

To obtain good results, however, a level of care is required as it has already been shown that such a synchronization system is vulnerable to a systematic frequency error [20], [25], [26], which can be unacceptably large when the power of the reference light is not high enough. Thus, the main goal of this article is to thoroughly discuss the effects occurring in the laser frequency synchronization circuits under low optical levels, present the background of the observed systematic error, provide analytic and simulation models, as well as discuss available countermeasures to keep this error under control. First, we present a short description of the basic laser frequency synchronization circuit.

II. Concept of Lasers Frequency Synchronization

The main idea behind the laser frequency synchronization circuit is shown in Fig. 2(a). Part of the reference light (ν_R) is combined with the light from the synchronized laser (ν_S) and produces a beat signal in the beat photodiode (PD). The beat frequency f_{BEAT}, equal to the difference $f_{\mathrm{BEAT}} = |\nu_R - \nu_S|$, is then processed in the laser stabilization subsystem, producing the signal controlling the frequency of the synchronized laser. Details of this block are sketched in Fig. 2(b). In practice, f_{BEAT} must match the dense wavelength-division multiplex (DWDM) grid [27]. Due to the availability of suitable optical filters the frequency offset can be either 12.5, 25, or 50 GHz. In the first step, such high frequency is downconverted to a more convenient intermediate value (selected to be around 2.6 GHz in the circuits discussed hereinafter), then bandpass filtered, and next divided down by NM in a divider chain, where the initial division is carried out by a fast prescaler. This divided frequency needs to

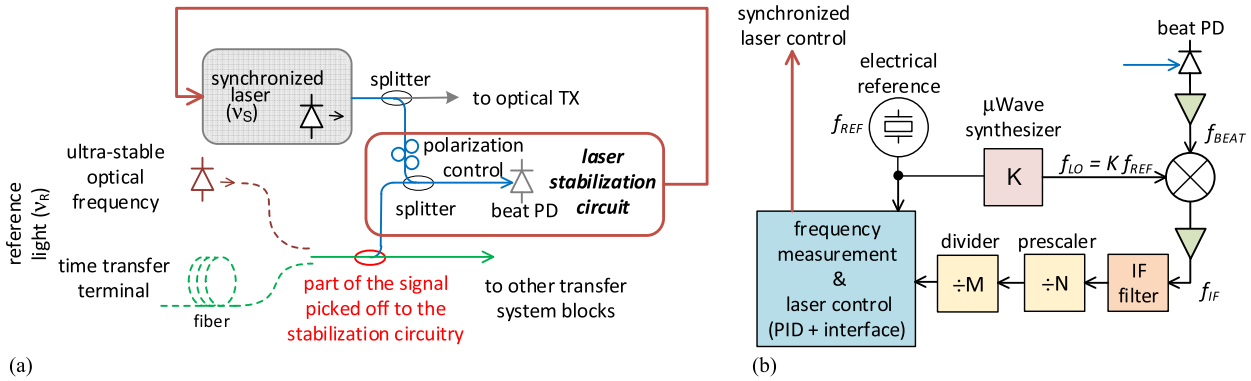

Fig. 2. (a) Idea of laser frequency synchronization and (b) details of the laser synchronization circuit.

be low enough to enable its counting using a timer/counter implemented in a microcontroller, which is also used to run a proportional–integral–derivative (PID) controller.

The offset frequency between the reference and the synchronized lasers $f_{\mathrm{BEAT}} = |\nu_R - \nu_S|$ can be found by analyzing the equilibrium condition in the feedback loop, which is formed by the synchronization system. It is equal to

$$f_{\mathrm{BEAT}} = NMf_{\mathrm{REF}} + f_{\mathrm{LO}} = (NM + K)\, f_{\mathrm{REF}} \tag{3}$$

where K is the multiplication factor of the microwave synthesizer used for the downconversion of the original beat signal. The frequency of the synchronized laser may be either higher or lower than ν_R, depending on the sign of the feedback loop gain.

III. Origin of Frequency Error at Low Optical Levels

The laser frequency synchronization circuit is a subsidiary of the entire fiber-optic transfer system, so it should be able to operate with a low optical input power, representing a small fraction of the reference light only. In such a case, the expected beat current is also low and the influence of the system noise becomes important. This noise can be assumed white and is composed of the shot noise of the light impinging the PD (mostly a relatively high power of the synchronized laser) and the thermal noise of the resistor (50 Ω) terminating the beat PD, with also a small contribution of the noise of the amplifiers and the mixer. It is assumed in all further considerations that the spectrum of the noise, which is distributed around f_{IF}, is limited by the IF filter whose passband is fully covered by the bandwidth of the prescaler, making the operation of the circuit greatly independent on the prescaler bandwidth. The noise affects the operation of the fast prescaler (i.e., the N divider), influencing the number of cycles counted in a reference time interval, which is used to estimate f_{BEAT}.

An example of such behavior is shown in Fig. 3, measured with the laser control fixed (i.e., with a feedback loop inactive). In Fig. 3(a), the case is shown when an optical power of around −40 dBm is applied as the reference light together with a power of about 5 dBm from the synchronized laser, producing substantial beat note, visible as a narrow peak in the spectrum at 2.6 GHz over the noise background. The spectrum of the noise was shaped by the filter with the noise bandwidth of about 1.5 GHz (BFCV-2610 + by Mini Circuits), which was followed by the prescaler rated for the operation up to 4 GHz (HMC988 by Hittite, configured as a by eight dividers). The output of the prescaler shows the square wave with the frequency of 325 MHz, which is an expected result. When the reference light is removed, however, leaving only noise as an input to the prescaler [see Fig. 3(b)], its output changes into a noisy waveform whose mean frequency is quite well defined (see Fig. 4 for the data for a few-day-long measurement, showing a mean frequency of about 322 MHz). One may thus expect that if the prescaler input power varies the mean, the output frequency of the prescaler also varies between two extremes—one corresponding to counting the pure signal (i.e., the desired frequency) and the other one corresponding to counting the pure noise, giving rise to a level-dependent systematic frequency error.

IV. Estimation of Prescaler Frequency Error

To get a deeper insight into the abovementioned error, we started from modeling the behavior of the prescaler treating it as a simple level-crossing detector driven by a time-continuous random process with a zero mean. Defining the number of zero crossings in a time interval of duration T as $\boldsymbol{n}(T)$, the mean frequency can then be expressed simply as $f_M = E\{\mathbf{n}(T)\}/2T$, where $E\{\cdot\}$ denotes an expectation (division by 2 is because both rising and falling edges are counted in this model). A known result from the level-crossing theory, which has been a subject of study for a long time, is that for a normal random process of power spectral density $S(f)$, the mean frequency is [29]

$$f_M = \sqrt{\int f^2 S(f)df \Big/ \int S(f)df}. \tag{4}$$

Applying (4) to the noise spectral density shown in Fig. 3(b) gives 2569 MHz, which is in a reasonably good agreement with the experimental value, equal to 2576 MHz (8 × 322 MHz). This result suggests that treating the prescaler as a level-crossing detector is a reasonable modeling approach, worth further investigation. Equation (4) can thus be used to determine the mean frequency corresponding to the band-limited noise, hereinafter referred to as f_{Mn}.

To tackle the problem when a sinusoidal component is also present, as such a process is no longer normal [29],

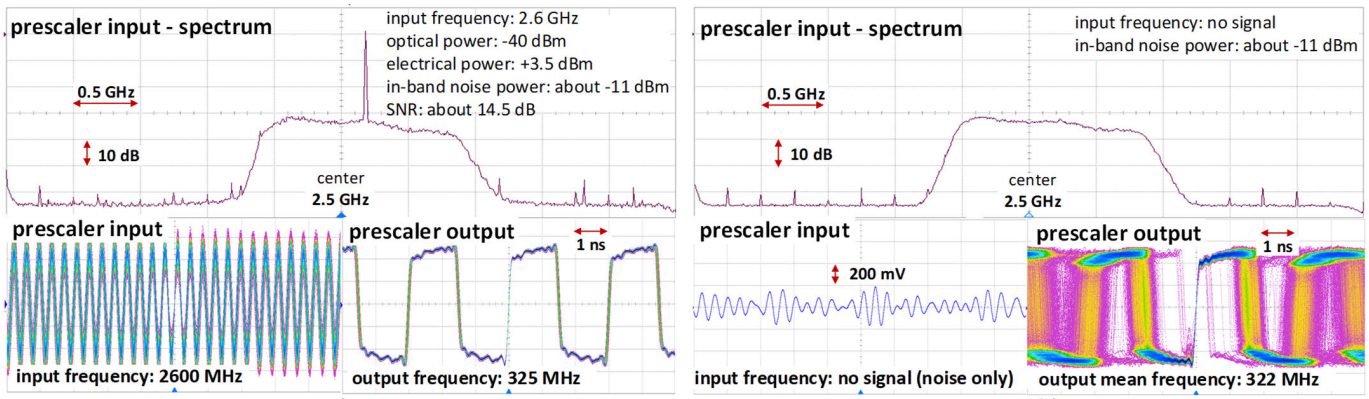

Fig. 3. Operation of the high-frequency prescaler in the presence of a band-limited noise with (a) high sinusoidal component at the input and (b) only the noise applied to the input.

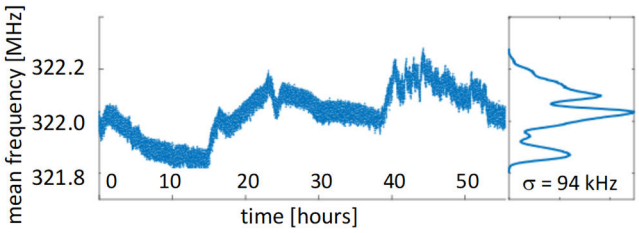

Fig. 4. Mean output prescaler frequency driven by a bandpass noise only. The fluctuations visible are due to environmental changes in a non-air-conditioned laboratory.

we decided to start with a simulation model developed in MATLAB. The model exploited is based on the same level-crossing approach discussed above. We used 2^{24} samples $\boldsymbol{x}[k]$ (k is the sample number) taken from the continuous signal composed of a pure sinusoid with frequency f_x and a band-limited normal noise with a power spectral density flat in the frequency range between f_L and f_H, where $f_L < f_x < f_H$. To determine the mean frequency, we counted a number of zero crossings in the entire vector $\boldsymbol{x}[k]$ by searching for the condition $\boldsymbol{x}[k]\boldsymbol{x}[k+1] < 0$. The amplitude of the sinusoidal component was varied as well as its frequency and we chose the parameters of the noise density to mimic the conditions shown in Fig. 3.

The results of the simulations are shown in Fig. 5(a) where a relative frequency error $\Delta f/f_x$, where $\Delta f = f_M - f_x$, is plotted versus the signal-to-noise ratio (SNR) for a few different values of the prescaler input frequency. As it can be seen, both the value and the sign of the error depend on the difference between f_x and f_{Mn}. When $f_x > f_{Mn}$ the error is negative and changes its sign to positive under the opposite condition. When f_x is located far from f_{Mn} and the SNR is low, the error can be huge—it can easily reach tens of megahertz. The error can be small, on the other hand, if $\approx f_x f_{Mn}$ is selected.

In Fig. 5(b) and (c), the results of simulations are compared with the experimental data obtained for a few high-speed prescalers (rated for the operation at a maximum frequency of 4, 6.5, and 12 GHz) for two different values of f_x shown in Fig. 5(a), equal to 2.16 and 3.12 GHz. It is evident from the presented plots that the choice of particular prescaler is not critical as all examined circuits show similar behavior. The agreement between the measurement and the simulation is also satisfactory—the real-world data show a slightly greater error than predicted from the simulation model, which is not surprising noting the model's simplicity. This is, however, interesting that such a simple model can still give reasonable results in a relatively large range of SNRs. As mentioned previously, the acceptable level of error in laser frequency synchronization circuits for ultraaccurate time-transfer links is about 5 MHz [25] that calls for relative error at the level around $2 \cdot 10^{-3}$ [shown with a dashed line in Fig. 5(b) and (c)]. To fulfill such a condition, the required SNR must be higher than some 8 dB in the presented examples and possibly even lower when f_x closer to f_{Mn} is selected (the question of the minimum required SNR will be addressed further in the text).

In addition to the simulation model (which requires substantial computation time), it would be desirable to have a formula allowing fast estimation of the systematic frequency error. The results available in the literature and known to the authors are, however, very general [28], [30] and cannot be directly applied. In this situation, an approximate solution may appear to be useful. A straightforward approach is to check whether (4) can be extended to the cases where both bandpass noise and a sinusoidal component are present in the spectrum entered in (4). Inserting the spectral density in the form $S(f) = S_n(f) + P_S\delta(f - f_x)$ into (4), where $S_n(f)$ is the noise spectrum (continuous) and the Dirac delta represents the sinusoidal component with power P_S and frequency f_x, and performing the required calculations gives the approximated mean frequency f_M^A in the form

$$f_M^A = \sqrt{\left(f_{Mn}^2 + f_x^2 \mathrm{SNR}\right)/(1+\mathrm{SNR})} \tag{5}$$

where $\mathrm{SNR} = P_S / \int S_n(f)df$ is the SNR.

The usefulness of the discussed approximation can be verified by comparing it with the results of the simulation. We assumed that $S_n(f)$ is uniformly distributed between the frequencies f_L and f_H. The comparison is shown in Fig. 6, where the simulation result f_M^S is marked with blue squares

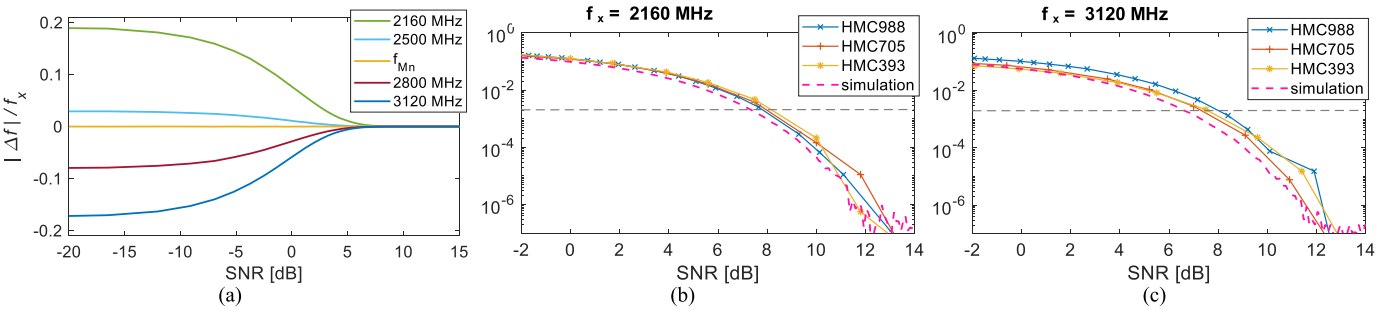

Fig. 5. Systematic frequency error caused by the presence of band-limited noise at the prescaler input: (a) simulation results and (b) and (c) comparison of the simulation with experimental data. $f_{Mn} = 2576$ MHz is assumed.

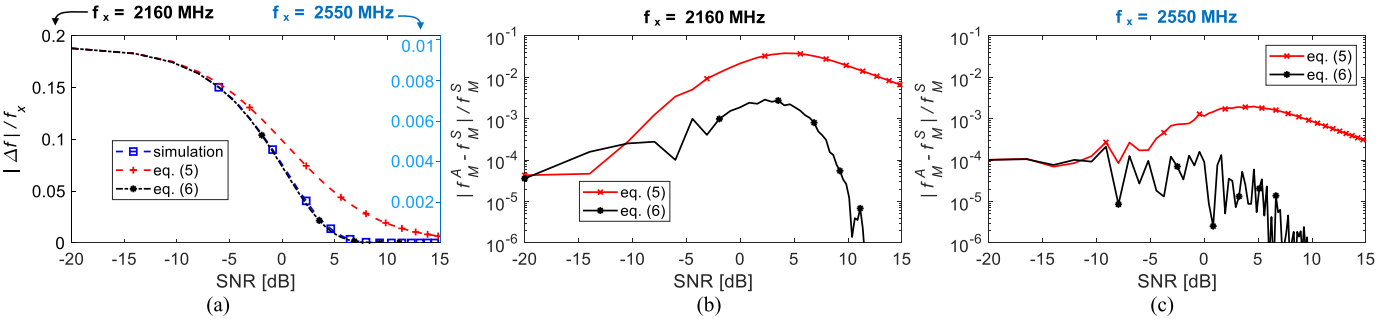

Fig. 6. Accuracy of approximation shown in (a) linear scale and (b) and (c) logarithmic scale using various approximation approaches. $f_{Mn} = 2576$ MHz is assumed.

and the approximation f_M^A is marked with red crosses. It is not surprising to see that the agreement is fairly good in a range of very low SNR where the noise dominates, making the prescaler input signal almost normal (thus, assumptions of (4) are almost satisfied). It deteriorates, however, in the more interesting range of the SNR where the sinusoidal component is dominating, even despite the fact that $f_M^A \to f_x$ when SNR $\to \infty$. This is because the signal driving the prescaler can now not be assumed to be normal, so the assumptions related to (4) are certainly violated. This deterioration is clearly visible in Fig. 6(b) where the logarithmic plot of the relative approximation accuracy, defined as $\left|f_M^A - f_M^S\right|/f_M^S$, is shown for $f_x = 2160$MHz as an example. Fortunately, the approximation accuracy improves if f_x is close to f_{Mn} [see Fig. 6(c)].

Looking for a means to further improve the approximation accuracy for SNR > 0 dB, we discovered that substituting $(\exp(\text{SNR}) - 1)$ for SNR in (5), resulting in

$$f_M^A = \sqrt{f_{Mn}^2 e^{-\text{SNR}} + f_x^2\left(1 - e^{-\text{SNR}}\right)} \tag{6}$$

allows obtaining much better results. The corresponding curves are shown in Fig. 6 with black lines, in both linear and logarithmic scales, and display that the modified formula (6) gains at least an order of magnitude improvement for SNR > 0 dB.

The change of the location of f_x with respect to f_{Mn} results in a change of the systematic frequency error, as it has already been mentioned [see Fig. 5(a)]. The curves presented in Fig. 6(a) appear to be universal so that, knowing the curve for some particular value f_{x1}, it can be converted into the curve for another value f_{x2} by scaling it by a factor equal to $f_{x1}/f_{x2}(f_{x2} - f_{Mn})/(f_{x1} - f_{Mn})$. This feature is shown in Fig. 6(a) where the scale at the right side was drawn assuming $f_x = 2550$ MHz (in this case, the abovementioned scaling factor equals about 0.05). In addition, (5) and (6) suggest that the discussed systematic frequency error can be expected to be independent on the specific shape of the noise spectrum $S_n(f)$, as the only noise-related parameter appears to be f_{Mn}.

V. Systematic Error in a Closed Feedback Loop

To determine the frequency error remaining after closing the feedback loop, it is helpful to consider the incremental model of the circuit from Fig. 2. In addition to the already discussed error Δf_N originating in the prescaler (defined here as $\Delta f_P = f_M - f_{\text{IFN}}$, where f_{IFN} is the nominal IF value, i.e., assuming no any prescaler frequency error), the model presented in Fig. 7(a) includes the inaccuracy of the electrical reference Δf_{REF}, which appears in two different places as this reference is used in the microwave synthesizer supplying f_{LO}, and also provides the time base for the beat note frequency counting by the timer/counter. All other error sources (as the laser noise $\Delta\nu_L$ and the quantization noise $\Delta\nu_Q$, which occurs when a digitally tuned integrated tuneable laser assembly—ITLA [31]—is used as the synchronized laser) are omitted now as not contributing to the systematic frequency error. H_L and H_P are the tuning sensitivity of the synchronized laser and the gain of the PID controller, respectively.

The noise-dependent incremental gain of the prescaler is defined as $\alpha = Ndf_{P\_O}/df_{P\_I}$, where f_{P_O} and f_{P_I} are the input and output prescaler frequencies, respectively. This parameter reflects the fact that the sensitivity of the prescaler to the change of its input frequency decreases when the SNR

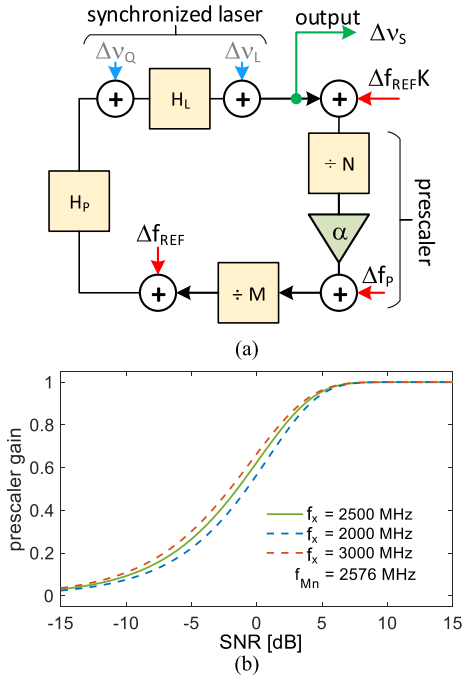

Fig. 7. (a) Incremental model of the laser frequency stabilization circuit and (b) prescaler incremental gain.

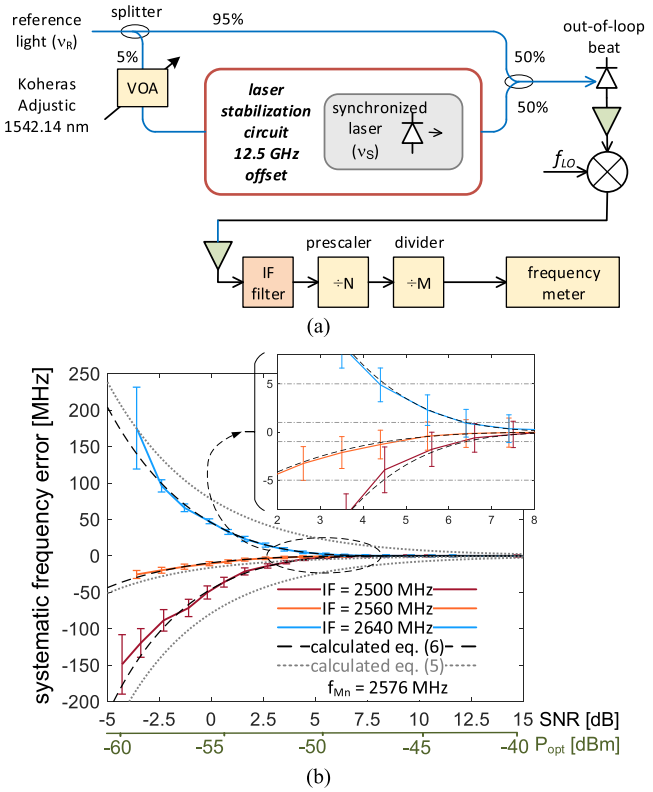

Fig. 8. (a) Setup for the out-of-loop measurement used to assess the systematic frequency error and (b) measurement results. The error bars show the measurement standard deviation.

decreases. It can be calculated using (6) as $\alpha = df_M^A(f_x)/df_x$. The relevant curves are shown in Fig. 7(b). It may be noted that α is relatively independent on f_x in the considered frequency range and is very close to one for SNR higher than about 5 dB. Its value decreases toward zero when the SNR is lowered.

Based on the feedback theory the incremental change of the synchronized laser frequency, $\Delta\nu_S$ can be cast in the form

$$\Delta\nu_S = \frac{\Delta f_P \frac{H_P H_L}{M} + \Delta f_{\mathrm{REF}} H_P H_L \left(1 + \frac{\alpha K}{MN}\right)}{1 + \frac{\alpha H_P H_L}{MN}}. \qquad (7)$$

Assuming that the loop gain, equal to $H_P H_L / MN$, is high due to the integrating part of the PID controller, (7) reduces in the limit to

$$\Delta\nu_S = \Delta f_P N/\alpha + \Delta f_{\mathrm{REF}} MN/\alpha + \Delta f_{\mathrm{REF}} K. \qquad (8)$$

The first term in (8) shows that in a closed feedback loop, the prescaler error, as shown in Fig. 5(a), scales inversely to the prescaler gain α and thus is effectively multiplied when the SNR is low. The inaccuracy of Δf_{REF} scales in a similar way, although this effect is much less pronounced because usually $MN\Delta f_{\mathrm{REF}} < \Delta f_P$. Assuming that a standard 10-MHz temperature compensated crystal oscillator (TCXO) is used with the inaccuracy of 2.5 ppm and that MN is in the order of 250 (as it is in the circuits, we investigated experimentally), $MN\Delta f_{\mathrm{REF}}$ not greater than 2.5 kHz may be expected, whereas Δf_N can be much larger, especially when the prescaler input frequency is far from f_{Mn} (see Fig. 5). The last term in (8) shows that the inaccuracy of Δf_{REF} transfers to the circuit output increased by the synthesizer's multiplication factor K. The error due to this can be expected not to be greater than about 10 kHz, as in the circuits with $f_{\mathrm{LO}} \approx 10$ GHz considered here, K around 1000 is required. In practice, therefore, one can expect that the systematic error will be dominated by the first term of (8) related to the prescaler.

To verify the predictions shown above, we performed the measurement of the systematic frequency error in the complete synchronization circuit using an out-of-loop configuration shown in Fig. 8(a) (the PD, amplifiers, mixer, IF filter, and prescaler used in the out-of-loop path were exactly the same as used in the stabilization circuit). The optical power from the reference laser (Koheras Adjustic X15) was split into two unequal parts with 5% directed to the synchronization circuit via a variable optical attenuator (VOA) to control the SNR at the input of the prescaler. The remaining 95% of the light was combined with the light produced by the synchronized laser and applied to an out-of-loop beat PD. The resulting signal was then processed by the circuit analogous to this used inside the laser stabilization circuit (composed of a beat PD, microwave amplifiers, mixers, and frequency dividers) and finally applied to the frequency counter (Pik Time T4100). Due to the high power of the out-of-loop beat signal, one can be sure that no any systematic frequency error occurred in the out-of-loop divider chain. Such a setup can thus be used to detect any difference from the intended 12.5-GHz offset between the reference light and the synchronized laser.

The results of the measurement are shown in Fig. 8(b) for a few values of the nominal intermediate frequencies f_{IFN} set by adjusting the microwave synthesizer inside the laser stabilization circuit. It is visible that when the SNR drops, the systematic offset starts to manifest—its expected

value (marked with black dashed lines) was obtained using (6) taking the calculated value with a negative sign (this is because the feedback loop tends to cancel out the error introduced by the prescaler causing the sign inversion) and scaling it by α according to (8). The calculations agree well with the measurements in all investigated cases confirming the applicability of the theoretical approach developed so far.

Fig. 8(b) (inset) shows an enlarged part of the curves where the error stays within ±5-MHz limit required for picosecond-accurate time-transfer systems. The required SNR values depend on the distance between f_{Mn} and the nominal f_{IFN} frequency. For f_{IFN} equal to 2560 MHz ($|f_{Mn} - f_{\mathrm{IFN}}| = 16$ MHz), an operation with an SNR down to about 2 dB is possible, whereas for larger distances, higher SNR is necessary.

VI. Minimum SNR and Required Signal Level

The minimum signal level required for the operation of the discussed laser synchronization circuits can be, in principle, determined by defining the acceptable level of the frequency error $\Delta\nu_{S\max}$. For the considered application of ultra-accurate time transfer, a value of $\Delta\nu_{S\max} = \pm 5$ MHz is adequate (see [25]), but it can be different for other applications. Knowing this, and also the value of f_{Mn}, which is specific for particular realization of the circuit, but can be quite easily measured with a frequency counter, one can choose a reasonable value of the nominal intermediate frequency f_{IFN} reasonably close to f_{Mn} (practical limit results from the long-term stability of f_{Mn}—see Fig. 4 for an example). The opposite approach when f_{Mn} is to be fit to the selected f_{IFN} is also possible, although it seems less convenient in practice, especially when rational microwave synthesizers are easily available. Having these data, it is possible to determine the required SNR by solving (6) under condition $f_M^A = f_{\mathrm{IFN}}$, forcing the output of the dividers chain to keep the frequency at the reference value due to the integrating part of the PID controller in the feedback loop. The solution takes the form

$$\begin{aligned}\mathrm{SNR} &= \ln\left(\left(f_{Mn}^2 - f_x^2\right)/\left(f_{\mathrm{IFN}}^2 - f_x^2\right)\right) \\ &\approx \ln\left(\left(f_{Mn} - f_{\mathrm{IFN}} + \Delta\nu_{S\max}\right)/\Delta\nu_{S\max}\right) \end{aligned} \tag{9}$$

where f_x was substituted with $f_{\mathrm{IFN}} + \Delta\nu_{S\max}$ (to get meaningful results, the sign of $\Delta\nu_{S\max}$ has to be positive for $f_{\mathrm{IFN}} > f_{Mn}$ and negative in the opposite case) and assuming typical working conditions ($\Delta\nu_{S\max} \ll f_{\mathrm{IFN}}$ and $f_{\mathrm{IFN}} \approx f_{Mn}$). As visible from (9), the result depends mostly on the difference $f_{Mn} - f_{\mathrm{IFN}}$, which is plotted in Fig. 9(a) for a few values of $\Delta\nu_{S\max}$.

To get the optical power corresponding to this particular SNR, more details of particular circuit implementation are required, such as the frequency characteristics of the IF filter and noise levels of the amplifiers and mixers used. For the circuits evaluated in the laboratory, the optical powers are shown in Fig. 8(b) where the range of the plot corresponds to the values from about −60 to −40 dBm. This shows that the circuit investigated experimentally is capable to operate within the acceptable systematic error level of 5 MHz with the input powers below −50 dBm.

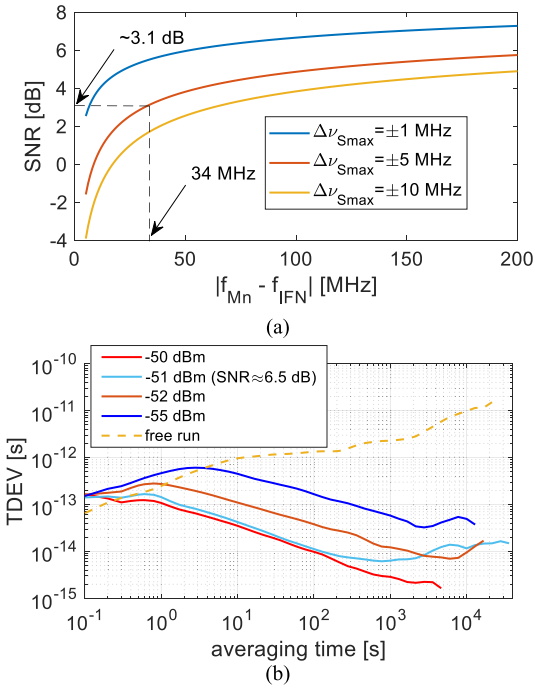

Fig. 9. (a) Minimum SNR required not to exceed $\Delta\nu_{S\max}$ and (b) TDEV calculated for a 1000-km-long fiber link based on the frequency stability measurements in the circuit with $f_{\mathrm{IFN}} = 2600$ MHz ($\approx |f_{Mn} - f_{\mathrm{IFN}}|$34 MHz).

The acceptable systematic error level, however, is not the only criterion that needs to be considered—a no less important factor is related to the deterioration of the stability of the output frequency ν_S with decreasing SNR and its influence on the stability of the time transfer. One reason for decreasing the feedback loop efficiency is suppressing the noise of the synchronized laser ($\Delta\nu_L$) and its tuning quantization ($\Delta\nu_Q$) because of decreasing the loop gain and bandwidth. The other reason is related to the multiplication of the prescaler noise. Both these effects are due to decrease of the prescaler gain α. This is shown in Fig. 8(b) by the vertical bars showing the standard deviation of the measured frequency. It may be noted that the standard deviation of the frequency increases with decreasing SNR. Nevertheless, this increase is smaller when selected f_{IFN} is closer to f_{Mn}.

The effect of the mentioned noise on the stability of the time transfer in a 1000-km-long fiber link using standard G.652 single-mode fiber with the chromatic dispersion coefficient of 17 $\mathrm{ps{\cdot}nm^{-1}\cdot km^{-1}}$ is shown in form of the time deviation (TDEV) in Fig. 9(b). In general, the curves for the optical power larger than −51 dBm (corresponding to the SNR of about +6.5 dB) are all very similar and close to the noise floor of the stabilization circuit and resulting mostly from the tuning quantization of the ITLA used in the experiment, which can be controlled with a coarse resolution of 1 MHz only (conforming with ITLA multisource agreement). For lower optical powers, however, noticeable deterioration of the TDEV curves is observed, roughly about 2–3 times per each dB. The decrease of the synchronization circuit bandwidth is also visible observing the change of the position of the bump appearing at the averaging time around 1 s.

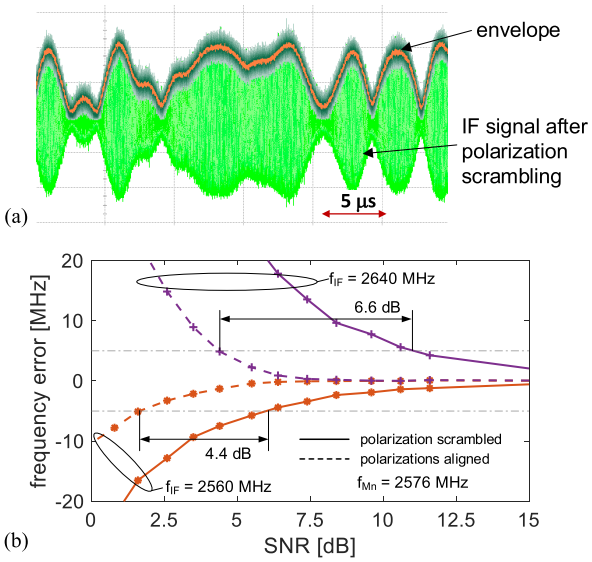

Fig. 10. Effect of polarization scrambling: (a) signal at the prescaler input and (b) frequency error due to scrambling with the scrambling penalty marked.

Stability deterioration due to decreasing input power (so SNR) will manifest also as increased jitter. For the cases shown above, the jitter contribution will be about 250 fs, 520 fs, and 1 ps for the input power greater than −51, −52, and −55 dBm, respectively. This suggests that both systematic frequency error and stability should be considered together and fit to particular requirements. For example, the comparison of Fig. 9(a) and (b) reveals that for the lowest TDEV and jitter, the input power should not fall below −51 dBm, which corresponds to SNR ≈ +6.5 dB. For the systematic error not exceeding ±5 MHz, the minimum required SNR about 3 dB lower should be enough on the other hand, but this time elevated jitter is to be accepted. Nevertheless, in any case, a substantial improvement with respect to TDEV of a free-running laser [shown with the dashed line in Fig. 9(b)] is well visible for almost all averaging times, which shows a clear advantage of the discussed laser stabilization circuits.

VII. Penalty Due to Polarization Scrambling

All the results discussed so far assumed that the polarizations of the fields beating at the PD are aligned. It was assured in the examined circuits using a polarization controller shown in Fig. 2(a). However, such a solution cannot work reliably in practice, as standard fibers change their polarization state randomly due to external factors such as temperature and mechanical stress variations [16]. A simple solution may be to use a polarization scrambler [16], [32], which is a stand-alone fiber-optic component, not requiring any additional feedback loop or control algorithms (in contrast to an adaptive polarization controller). However, the polarization scrambler reduces the average power of the beat by 3 dB, resulting in a modulation of the IF signal level driving the prescaler [see Fig. 10(a)]. In this way, the instantaneous SNR is affected, resulting in a systematic frequency error, according to the discussion in Sections III, IV, and VI.

The effect of polarization scrambling is shown in Fig. 10(b) (solid lines) for two different f_{IFN} values. It is noticeable that scrambling brings with it the disadvantage of increased SNR required to recover the same value of systematic frequency error without scrambling (dashed lines). In the examples shown, the penalty is either 4.4 or 6.6 dB depending on the difference between f_{IFN} and f_{Mn}. Once again, it can be seen that it is advantageous to choose f_{IFN} close to f_{Mn} in order to minimize the disadvantage.

The minimum scrambling penalty of 3 dB should be expected due to the decrease of IF signal level mentioned above. The theoretical prediction of the penalty can in principle be made by averaging the frequency over all instantaneous SNR values, ranging from the minimum for orthogonal polarizations to the maximum for parallel polarizations. However, it is difficult to obtain accurate and meaningful results because such a procedure is sensitive to the SNR distribution and cannot be held stable or approximated reliably.

VIII. Conclusion

The circuits developed here for synchronization of a semiconductor laser frequency to a weak optical reference from a remote laser allow a substantial reduction of the calibration uncertainty related to the chromatic dispersion in fiber-optic time-transfer systems. However, the systematic frequency error that occurs in such circuits must be kept under control. This error discussed in detail in the text arises in the first stage of the frequency divider chain (so-called prescaler) due to the band-limited noise interfering with the sinusoidal component, whose frequency is estimated by counting the number of slopes in a reference time interval. Due to the experimental work carried out, the simulations, and theoretical models, we can state that the value of the prescaler error is directly related to the SNR at the prescaler input and the difference between the frequency of the sinusoidal component and the mean frequency corresponding only to the counting the bandpass noise (designated as f_{Mn} in the text). Despite the noisy character of the prescaler output under such conditions (i.e., driven by the bandpass noise), the mean frequency observed at the prescaler output appears to be well defined and fairly stable. It is thus a reliable parameter, useful in characterizing circuits with prescalers. The value of this frequency can be easily determined, either based on the input noise spectrum or by direct measurement.

If the prescaler is part of a feedback loop used to bring the frequency of a stabilized laser closer to the frequency of the optical reference light, the systematic frequency error is multiplied by the reciprocal of the prescaler gain α, which is close to one for SNR higher than about 5 dB, but drops gradually to zero for lower values. At low SNR, the systematic frequency errors have thus a tendency to increase very rapidly. With the methods described in the text, it is possible to predict the error value or determine the required SNR to keep the error below an arbitrarily chosen value. According to the results presented, operation with an SNR down to a few dB is reliably possible in the experimentally examined circuits. The conditions are substantially relaxed when the circuit is operated near to the mean frequency determined by the prescaler input noise f_{Mn}. A look at Fig. 4, showing the

long-term behavior of f_{Mn} under realistic conditions, shows that the difference between f_{Mn} and the nominal IF f_{IFN} can be chosen to be below 1 MHz.

Operation close to f_{Mn} is also helpful when the polarization scrambling is implemented to avoid polarization alignment problems. In such a case, as shown experimentally, the scrambling penalty can be kept only slightly higher than the theoretical minimum of 3 dB.

REFERENCES

[1] J. Guéna et al., "First international comparison of fountain primary frequency standards via a long distance optical fiber link," *Metrologia*, vol. 54, no. 3, pp. 348–354, 2017, doi: 10.1088/1681-7575/aa65fe.

[2] P. Delva et al., "Test of special relativity using a fiber network of optical clocks," *Phys. Rev. Lett.*, vol. 118, Jun. 2017, Art. no. 221102, doi: 10.1103/PhysRevLett.118.221102.

[3] W. F. McGrew et al., "Towards the optical second: Verifying optical clocks at the SI limit," *Optica*, vol. 6, no. 4, pp. 448–454, 2019, doi: 10.1364/OPTICA.6.000448.

[4] P. Morzyński et al., "Absolute measurement of the $^1S_0$-$^3P_0$ clock transition in neutral ^{88}Sr over the 330 km-long stabilized fibre optic link," *Sci. Rep.*, vol. 5, p. 17495, Dec. 2015, doi: 10.1038/srep17495.

[5] B. Wang et al., "Square kilometre array telescope—Precision reference frequency synchronisation via 1f-2f dissemination," *Sci. Rep.*, vol. 5, p. 13851, Sep. 2015, doi: 10.1038/srep13851.

[6] C. Clivati et al., "A VLBI experiment using a remote atomic clock via a coherent fibre link," *Sci. Rep.*, vol. 7, p. 40992, Feb. 2019, doi: 10.1038/srep40992.

[7] P. Krehlik et al., "Fibre-optic delivery of time and frequency to VLBI station," *Astron. Astrophys.*, vol. 603, p. A48, Jul. 2017, doi: 10.1051/0004-6361/201730615.

[8] T. E. Mehlstäubler, G. Grosche, C. Lisdat, P. O. Schmidt, and H. Denker, "Atomic clocks for geodesy," *Rep. Prog. Phys.*, vol. 81, no. 6, Jun. 2018, Art. no. 064401, doi: 10.1088/1361-6633/aab409.

[9] Ł. Śliwczyński, "Calibrated optical time transfer of UTC(k) for supervision of telecom networks," *Metrologia*, vol. 56, no. 1, 2019, Art. no. 015006, doi: 10.1088/1681-7575/AAEF57.

[10] Ł. Śliwczyński, "Fiber-based UTC dissemination supporting 5G telecommunications networks," *IEEE Commun. Mag.*, vol. 58, no. 4, pp. 67–73, Apr. 2020, doi: 10.1109/MCOM.001.1900599.

[11] P. Tavella and G. Petit, "Precise time scales and navigation systems: Mutual benefits of timekeeping and positioning," *Satell. Navigat.*, vol. 1, no. 1, p. 10, Dec. 2020, doi: 10.1186/s43020-020-00012-0.

[12] A. Derviskadic, R. Razzaghi, Q. Walger, and M. Paolone, "The white rabbit time synchronization protocol for synchrophasor networks," *IEEE Trans. Smart Grid*, vol. 11, no. 1, pp. 726–738, Jan. 2020, doi: 10.1109/TSG.2019.2931655.

[13] J. Lopez-Jimenez, J. L. Gutierrez-Rivas, E. Marin-Lopez, M. Rodriguez-Alvarez, and J. Diaz, "Time as a service based on white rabbit for finance applications," *IEEE Commun. Mag.*, vol. 58, no. 4, pp. 60–66, Apr. 2020, doi: 10.1109/MCOM.001.1900602.

[14] M. Lombardi, "An evaluation of dependencies of critical infrastructure timing systems on the global positioning systems (GPS)," NIST, Gaithersburg, MD, USA, Tech. Note 2189, 2020, doi: 10.6028/NIST.TN.2189.

[15] P. Krehlik, Ł. Śliwczyński, Ł. Buczek, J. Kołodziej, M. Lipiński, "ELSTAB—Fiber-optic time and frequency distribution technology: A general characterization and fundamental limits," *IEEE Trans. Ultrason., Ferroelectr., Freq. Control*, vol. 63, no. 7, pp. 993–1004, Jul. 2016, doi: 10.1109/TUFFC.2015.2502547.

[16] O. Lopez, A. Amy-Klein, M. Lours, C. Chardonnet, and G. Santarelli, "High-resolution microwave frequency dissemination on an 86-km urban optical link," *Appl. Phys. B, Lasers Opt.*, vol. 98, no. 4, pp. 723–727, Mar. 2010, doi: 10.1007/s00340-009-3832-1.

[17] Q. Li, L. Hu, J. Chen, and G. Wu, "Studying the double Rayleigh backscattering noise effect on fiber-optic radio frequency transfer," *IEEE Photon. J.*, vol. 13, no. 2, Apr. 2021, Art. no. 7100210, doi: 10.1109/JPHOT.2021.3058171.

[18] J. Gersl, P. Delva, and P. Wolf, "Relativistic corrections for time and frequency transfer in optical fibres," *Metrologia*, vol. 52, no. 4, pp. 552–564, 2015, doi: 10.1109/EFTF.2014.7331477.

[19] R. Szplet, R. Szymanowski, and D. Sondej, "Measurement uncertainty of precise interpolating time counters," *IEEE Trans. Instrum. Meas.*, vol. 68, no. 11, pp. 4348–4356, Nov. 2019, doi: 10.1109/TIM.2018.2886940.

[20] Ł. Śliwczyński, P. Krehlik, Ł. Buczek, and H. Schnatz, "Picoseconds-accurate fiber-optic time transfer with relative stabilization of lasers wavelengths," *J. Lightw. Technol.*, vol. 38, no. 18, pp. 5056–5063, Sep. 15, 2020, doi: 10.1109/JLT.2020.2999158.

[21] S. Raupach and G. Grosche, "Chirped frequency transfer: A tool for synchronization and time transfer," *IEEE Trans. Ultrason., Ferroelectr., Freq. Control*, vol. 61, no. 6, pp. 920–929, Jun. 2014, doi: 10.1109/TUFFC.2014.2988.

[22] O. Lopez et al., "Simultaneous remote transfer of accurate timing and optical frequency over a public fiber network," *Appl. Phys. B, Lasers Opt.*, vol. 110, no. 1, pp. 3–6, 2013, doi: 10.1109/EFTF-IFC.2013.6702214.

[23] P. Krehlik, H. Schnatz, and Ł. Śliwczyński, "A hybrid solution for simultaneous transfer of ultrastable optical frequency, RF frequency, and UTC time-tags over optical fiber," *IEEE Trans. Ultrason., Ferroelectr., Freq. Control*, vol. 64, no. 12, pp. 1884–1890, Dec. 2017, doi: 10.1109/TUFFC.2017.2759001.

[24] X. Tian, L. Hu, G. Wu, and J. Chen, "Hybrid fiber-optic radio frequency and optical frequency dissemination with a single optical actuator and dual-optical phase stabilization," *J. Lightw. Technol.*, vol. 38, no. 16, pp. 4270–4278, Aug. 15, 2020, doi: 10.1109/JLT.2020.2989328.

[25] Ł. Śliwczyński, P. Krehlik, Ł. Buczek, and H. Schnatz, "Synchronized laser modules with frequency offset up to 50 GHz for ultra-accurate long-distance fiber optic time transfer links," *J. Lightw. Technol.*, vol. 40, no. 9, pp. 2739–2747, May 1, 2022, doi: 10.1109/JLT.2022.3147591.

[26] Ł. Śliwczyński, P. Krehlik, and Ł. Buczek, "Noise limit on the accuracy of frequency locking of lasers for ultra-acurate fiber-optic time transfer," in *Proc. Joint Conf. Eur. Freq. Time Forum IEEE Int. Freq. Control Symp. (EFTF/IFCS)*, Paris, France, vol. 5133, Apr. 2022, pp. 24–28 doi: 10.1109/EFTF/IFCS54560.2022.9850558.

[27] *Spectral Grids for WDM Applications: DWDM Frequency Grid*, document Recommendation ITU-T G.694.1, International Telecommunication Union, 2020.

[28] D. Middleton, *An Introduction to Statistical Communication Theory*. Piscataway, NJ, USA: IEEE Press, 1996, pp. 426–435.

[29] A. Papoulis, *Probability, Random Variables and Stochastic Processes*, 3rd ed. New York, NY, USA: McGraw-Hill, 1991, pp. 603–612.

[30] W. Davenport and W. Root, *An Introduction to the Theory of Random Signals and Noise*. New York, NY, USA, IEEE Press, 1987, pp. 165–167.

[31] *Integrable Tunable Laser Assembly Multi Source Agreement*, document OIF-ITLA-MSA-01.3 Implementation Agreement, Optical Internetworking Forum, 2015.

[32] D. Xu, O. Lopez, A. Amy-Klein, and P.-E. Pottie, "Polarization scramblers to solve practical limitations of frequency transfer," *J. Lightw. Technol.*, vol. 39, no. 10, pp. 3106–3111, May 15, 2021, doi: 10.1109/JLT.2021.3057804.